Journal of Al-Azhar University Engineering Sector

Vol.20, No. 77, October 2025, 1324 - 1342

EXPERIMENTAL INVESTIGATION OF A NOVEL SAVONIUS TURBINE WITH PARTIALLY FLEXIBLE BUCKETS

Mohamed Elsakka[1,2,*], Abdulrahman Muftah[1], Ahmed Amer[1], Ahmed Refaat[2,3], Ayman Mohamed[1], Asmaa Ahmed[1,2]

[1] Mechanical Power Engineering Department, Faculty of Engineering, Port Said University, Egypt

[2] Faculty of Engineering, East Port Said National University, Salam Misr City, East Port Said, Egypt

[3] Electrical Engineering Department, Faculty of Engineering, Port Said University, Egypt

***Correspondance:** elsakka@eng.psu.edu.eg

Citation:

M. Elsakka, A. Muftah, A.Amer, A. Refaat, A. Mohamed, A. Ahmed" Experimental Investigation of A Novel Savonius Turbine With Partially Flexible Buckets ", Journal of Al-Azhar University Engineering Sector, vol. 20(77), pp. 1324-1342, 2025

Received: 20 June 2025

Revised: 02 August 2025

Accepted: 16 August 2025

Doi: 10.21608/auej.2025.405164.1896

ABSTRACT

Savonius wind turbines, due to their drag-based operation, generally exhibit low aerodynamic efficiency, prompting ongoing efforts to improve their performance in low-wind-speed environments.This study investigates the use of partially flexible buckets, featuring passive morphing fabric sections, to enhance torque generation and power output without increasing mechanical complexity. Flexible bucket geometries were characterized using two dimensionless parameters: the Sagitta Ratio (SR), describing surface curvature, and the Flexible Ratio (FR), representing the deformable region's span. A series of experimental tests was conducted in an open-jet wind tunnel under controlled conditions, comparing flexible configurations to a rigid baseline across varying tip speed ratios (TSRs). Results show that all flexible designs retained self-starting capability, with performance highly dependent on the SR–FR combination. The optimal configuration (SR = 0.2, FR = 0.5) achieved a peak power coefficient (Cp) of 12.9%, surpassing the rigid reference Cp of 12.2%, and reached steady-state rotation in 24.8 seconds, faster than the 28.3 seconds required by the rigid turbine. These findings demonstrate that judicious use of passive flexibility can enhance Savonius turbine performance while preserving simplicity and structural integrity. The study offers a viable path toward low-cost, scalable wind energy solutions for decentralized and urban applications.

KEYWORDS: Savonius wind turbine, Wind tunnel, Torque meter, Passive morphing, Flexible bucket

التحقيق التجريبي لتوربين سافونيوس جديد مزوَّد بدلاء مرنة جزئيًا

محمد السقا[١،٢،*]، عبد الرحمن مفتاح[١]، أحمد عامر[١]، أحمد رفعت[٢،٣]، أيمن محمد[١]، أسماء أحمد[١،٢]

[١] قسم هندسة القوى الميكانيكية، كلية الهندسة، جامعة بورسعيد، مصر

[٢] كلية الهندسة، جامعة شرق بورسعيد الأهلية، مدينة سلام مصر، شرق بورسعيد، مصر

[٣] قسم الهندسة الكهربية، كلية الهندسة، جامعة بورسعيد، مصر

البريد الالكتروني للباحث الرئيسي: elsakka@eng.psu.edu.eg

الملخص

تُعد الكفاءة الديناميكية الهوائية لتوربينات الرياح من نوع سافونيوس محدودة بطبيعتها بسبب اعتمادها على مقاومة الهواء، مما يدفع إلى البحث عن تصاميم مبتكرة لتحسين الأداء في بيئات منخفضة السرعة الهوائية. تهدف هذه الدراسة إلى تحسين توليد العزم والقدرة من خلال استخدام دلاء مرنة جزئيًا تحتوي على مناطق نسيجية قابلة للتشكل بشكل سلبي، دون زيادة التعقيد الميكانيكي للتوربين. تم توصيف أشكال الدلاء المرنة باستخدام معاملين غير بُعديين: نسبة السَّهم (SR) التي تصف انحناء السطح، ونسبة المرونة (FR) التي تمثل الامتداد الطولي للمنطقة القابلة للتشكل. أُجريت سلسلة من التجارب داخل نفق هوائي مفتوح في ظروف محكمة، حيث تم مقارنة التكوينات المرنة مع نموذج مرجعي صلب عبر نسب سرعة طرفية مختلفة.(TSR)

أظهرت النتائج أن جميع التكوينات المرنة حافظت على القدرة الذاتية على بدء الدوران، مع اعتماد الأداء بشكل كبير على تآزر معامليSR و FR. وقد حقق التكوين الأمثل (FR=0.5, SR=0.2) أعلى معامل قدرة (Cp) بلغ ١٢,٩٪، متفوقًا على النموذج الصلب الذي بلغ Cp له ١٢,٢٪، كما بلغ وقت الوصول إلى حالة الدوران المستقرة ٢٤,٨ ثانية مقارنة بـ ٢٨,٣ ثانية في النموذج الصلب. تؤكد هذه النتائج أن الاستخدام المدروس للمرونة السلبية يمكن أن يعزز أداء توربينات سافونيوس، مع الحفاظ على البساطة وسلامة الهيكل. وتقدم الدراسة مسارًا واعدًا نحو حلول طاقة رياح منخفضة التكلفة وقابلة للتوسع، خاصة في التطبيقات اللامركزية والحضرية.

الكلمات المفتاحية : توربين رياح سافونيوس، نفق هوائي، جهاز قياس العزم، التحوّل السلبي في الشكل، ريشة مرنة.

1. INTRODUCTION

The global transition toward sustainable energy has become imperative in the face of escalating climate change, depleting fossil fuel reserves, and the pressing need to decarbonize electricity generation. Among renewable sources, wind energy stands out for its maturity, scalability, and minimal environmental footprint. While horizontal-axis wind turbines (HAWTs) dominate utility-scale installations, their dependency on high, consistent wind speeds and complex yaw systems limits their deployment in urban, off-grid, or low-wind environments. In contrast, vertical-axis wind turbines (VAWTs) offer greater adaptability for decentralized power generation due to their omnidirectional wind acceptance, compact form, and ease of maintenance [1, 2].

Among VAWTs, the Savonius turbine has garnered particular interest for its simple design, low manufacturing cost, and strong self-starting capability at low wind speeds. Operating primarily through differential drag, Savonius turbines are well-suited for rooftops, remote areas, and small-scale energy systems. Yet, this simplicity entails low aerodynamic efficiency, with typical power coefficients (C_p) ranging from 0.15 to 0.30—well below the Betz limit and significantly inferior to lift-based counterparts such as Darrieus rotors [3, 4]. To address this, numerous passive design modifications have been proposed: adjusting bucket count, aspect ratio, overlap ratio, end-plate geometry, and employing multi-stage stacks [5-8], as well as external flow augmenters like guide vanes, nozzles, and deflectors [9, 10]. Among these innovations, the introduction of bucket slots or vents has been particularly effective at improving performance through pressure modulation.

Computational Fluid Dynamics (CFD) was employed to show that small-slot placements near the leading edge significantly boost static and dynamic torque by preserving pressure differentials [11]. These findings were validated experimentally, demonstrating that a 5° slot angle offers peak C_p at low wind speeds [12]. The parameter space was expanded to explore overlap ratios and slot configurations, and an optimal $C_p \approx 0.138$ was found at TSR ≈ 0.526 [13]. CFD and Taguchi methods were applied to hydrokinetic analogues, pinpointing slot-gap width as the most influential factor [14]. An experimental investigation was conducted on multi-staged Savonius rotors with modified-Bach blades and check valves, demonstrating that adding a valve near the blade tip significantly improved both the power and static torque coefficients [15]. Although multi-staging helped reduce torque fluctuations, the associated drop in power coefficient was offset by the valve addition, which enabled a two-stage rotor to surpass the performance of a single-stage configuration by 4% [15]. The effect of automatic valves placed at different positions along the blade was also evaluated, showing that positioning the valve at the blade tip reduced the negative torque from the returning blade and increased the power coefficient by 20.8%, while valves near the rotor axis or center had adverse effects [16].

Recent research efforts have focused on improving the aerodynamic performance of Savonius wind turbines by introducing flexible bucket designs that adapt to the flow during operation. These designs aim to reduce the negative torque produced by the returning bucket while enhancing the positive torque from the advancing one, thereby increasing the overall power coefficient. A Savonius turbine with partially deformable blades featuring a flexible trailing edge that expands during rotation to form an active slot was investigated, improving pressure distribution and enhancing torque generation [17]. Two-dimensional CFD simulations showed up to a 32% increase in torque coefficient for larger deformation amplitudes, but smaller amplitudes were found to reduce performance, highlighting that although flexibility improved torque in certain cases, it could lead to a decrease in power coefficient under suboptimal deformation conditions [17]. A flexible geometry Savonius turbine with an eccentric bucket path was introduced by mounting the blades on a sliding guide track system connected to the turbine’s endplates, allowing the blades to deform elastically depending on their angular position and dynamically alter the turbine's active area [18]. The influence of eccentricity ratios (5% to 15%) was numerically examined using coupled structural-flow simulations, showing improvements in power coefficient by up to 90% compared to a rigid configuration [19]. The flexible design was also found to reduce the tip speed ratio (TSR) at which peak performance occurs, shifting it from 1.1 to 0.9 and achieving a maximum power coefficient of 0.412 [20]. This highlights the suitability of such turbines for low-wind-speed environments, especially in urban settings. A mechanically feasible Savonius turbine design featuring hinged, deformable blades that follow non-coaxial guide grooves was also introduced, allowing the blade shape to adapt passively with rotation angle [21]. This configuration eliminates the need for active actuators while still enabling significant aerodynamic enhancement, with numerical simulations showing that moderate deformation amplitudes improved the torque coefficient by 24%, while full-radius deformation (R_1) achieved gains up to 90.6%, with peak performance at TSR = 1 [21]. Despite these promising outcomes, the design still relies on precise mechanical alignment, which may affect durability and maintenance in real-world conditions, and the absence of experimental validation underscores the need for practical testing and refinement to ensure long-term reliability and scalability [21].

These studies collectively underscore the potential of flexible or morphing bucket designs to significantly enhance both static and dynamic torque, particularly in low tip-speed ratio (TSR) regimes—conditions well-suited for urban and remote wind energy applications. However, a common limitation across many of these designs is their mechanical complexity, often involving components such as hinges, valves, articulated linkages, or membranes. These additions can compromise system reliability, increase production costs, and complicate maintenance. Moreover, the majority of prior research remains predominantly numerical, with limited experimental validation and few direct comparisons against conventional rigid-bucket configurations under realistic operating conditions.

To address these gaps, the present study proposes and experimentally evaluates a novel Savonius turbine design featuring partially flexible buckets that demonstrate passive morphing behavior. The flexible section of each bucket is formed using an artificial silk fabric, sewn to create a concave, canopy-like surface—similar in form and behavior to a parachute. This fabric section responds passively to aerodynamic forces: compressing during the return stroke to reduce drag, and expanding during the advancing stroke to increase the effective frontal area. Crucially, this shape adaptation is achieved without any active control systems or mechanically complex components.

Wind tunnel tests are conducted under controlled conditions to assess both the startup performance and aerodynamic efficiency of the proposed design. Results are benchmarked against a rigid-bucket baseline to quantify improvements in torque generation and power coefficient across a range of TSRs. These findings provide new experimental evidence supporting the use of passive morphing in drag-based turbines and demonstrate the feasibility of low-cost, mechanically simple Savonius designs for decentralized and low-wind-speed energy applications.

2. GEOMETRIC PARAMETERIZATION OF THE FLEXIBLE BUCKET

The proposed flexible portion of the bucket is constructed from artificial silk fabric, sewn into a concave, canopy-like shape—resembling the form and behavior of a parachute. The flexible bucket material is a high-strength silk fabric widely used in tents, umbrellas, and other outdoor applications, chosen for its proven durability, tear resistance, and flexibility under cyclic loading. The depth of this concavity plays a crucial role in governing the deformation characteristics of the bucket and, in turn, significantly influences its aerodynamic performance. This includes effects on drag generation, flow separation, and overall power coefficient. To systematically describe and quantify the geometry of the flexible, concave surface, the concept of sagitta is employed.

The sagitta (also known as the versine) is defined as the perpendicular distance between the midpoint of a chord and the corresponding arc of a circle, as illustrated in **Fig. 1**. The sagitta is normalized by the chord length to form the sagitta ratio (SR), which is used in this study to characterize the shape and deformation behavior of the flexible bucket. For a circular arc with radius r, a chord of length c, and a sagitta s, the SR is given by:

$$SR = \frac{s}{c} = \frac{r}{c} - \sqrt{\left(\frac{r}{c}\right)^2 - 1/4} \tag{1}$$

This non-dimensional parameter (SR) provides a consistent and scalable way to describe the degree of concavity in the bucket's flexible surface, and is varied systematically in this study to assess its impact on turbine performance.

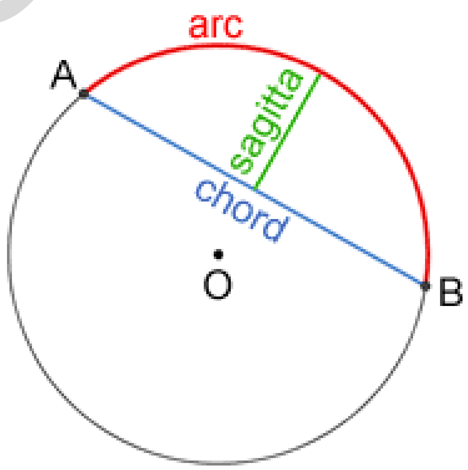

Fig. 1: Geometric definition of the sagitta (versine) as the perpendicular distance from the midpoint of a chord to the corresponding arc of a circle

The size of the flexible portion of the bucket plays a significant role in shaping the deformation behavior of the bucket and, consequently, the overall performance of the turbine. To quantify this aspect, the flexible ratio (FR) is introduced. It is defined as the ratio between the diameter-wise width of the flexible region and the overall diameter of the turbine. This non-dimensional parameter provides a convenient means to parameterize the relative extent of flexibility applied to the bucket structure and is used in this study to assess its influence on aerodynamic behavior and energy conversion efficiency.

Fig. 2 illustrates a two-dimensional representation of the combined effects of both the sagitta ratio (SR) and the flexible ratio (FR) on the shape of the concave flexible portion of the bucket. The diagram includes various combinations of FR values (0.4, 0.5, and 0.6) and SR values (0.1, 0.2, and 0.3), showing how each parameter influences the curvature and extent of the flexible surface. As shown in **Fig. 2(b)**, an SR of 0.3 at an FR of 0.5 results in a curvature that closely approaches tangency with the fixed (rigid) part of the bucket. This near-tangential profile suggests that increasing the SR beyond 0.3 under these conditions may be counterproductive.

As SR increases from 0.1 to 0.3 for a given FR, the concavity becomes more pronounced, indicating a deeper canopy-like deformation. Likewise, increasing FR from 0.4 to 0.6 leads to a wider flexible region across the bucket's diameter, further modifying its aerodynamic profile. To better visualize the spatial form of these deformations, **Fig. 3** presents the corresponding three-dimensional geometries of the flexible bucket configurations for the same SR and FR combinations. These geometric variations underscore the critical influence of SR and FR on the deformation behavior and potential aerodynamic performance of the flexible bucket, which is further investigated in the experimental analysis that follows.

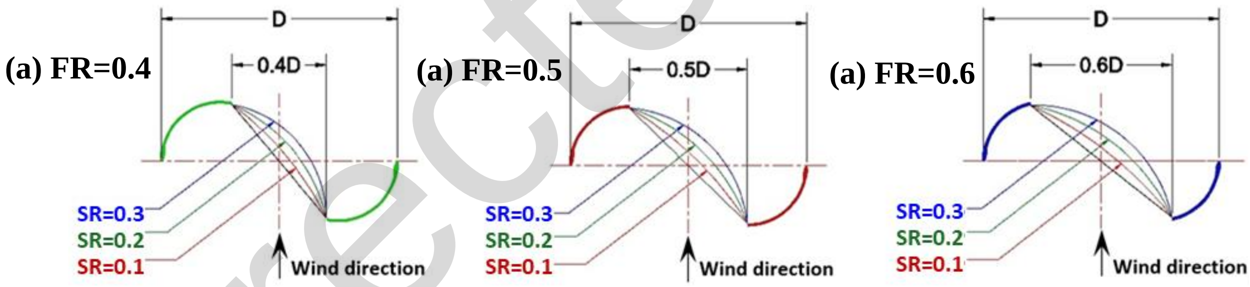

Fig. 2: Parametric 2D illustration of the influence of various combinations of sagitta ratio (SR = 0.1, 0.2, 0.3) and flexible ratio (FR = 0.4, 0.5, 0.6) on the curvature and extent of the flexible surface of the Savonius bucket

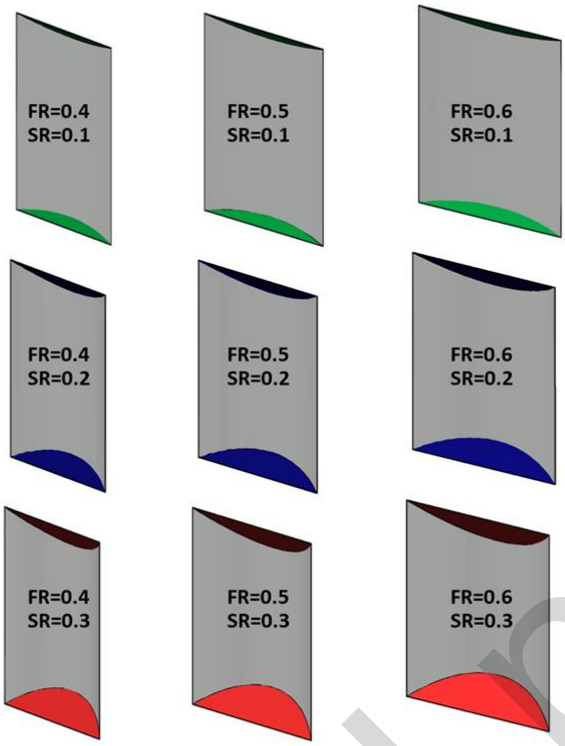

Fig. 3: Three-dimensional representations of the flexible portion of the bucket geometry for various combinations of sagitta ratio (SR = 0.1, 0.2, 0.3) and flexible ratio (FR = 0.4, 0.5, 0.6). The figure illustrates how the curvature and overall shape of the concave flexible surface vary in response to changes in these design parameters

3. METHODOLOGY

This study experimentally investigates the aerodynamic performance of a Savonius vertical-axis wind turbine (VAWT) equipped with partially flexible buckets. All tests were carried out under controlled laboratory conditions using the open-jet wind tunnel facility at Port Said University.

The wind tunnel system is driven by two identical 5.5 kW centrifugal blowers, each delivering airflow through an independent branch connected via flexible joints. In each branch, the airflow passes through two wide-angle diffusers arranged in series. A porous screen is installed between the diffusers to promote uniformity, while a second screen at the exit of the final diffuser provides additional flow stabilization. The flows from both branches merge into a common settling chamber, followed by a contraction section that accelerates and further refines the airstream before it enters the test section.

The test section has a cross-sectional area of 60 cm × 60 cm and provides a uniform velocity profile across a wind speed range of 3–17 m/s, making it well-suited for evaluating small-scale wind turbine configurations. With a rotor swept area of 0.09 m^2 and a test section area of 0.36 m^2, the resulting blockage ratio is approximately 25%, which is within the acceptable range for open-jet wind tunnel setups. At this blockage level, wall interference effects are minimal and do not significantly impact measurement accuracy [23]. A schematic of the optimized wind tunnel configuration is presented in **Fig. 4**, and additional technical specifications are provided in [22].

The rigid components of the turbine prototypes were fabricated using PLA+ material via 3D printing, based on CAD models developed in AutoCAD. Several configurations were tested, including a rigid baseline model and multiple variants featuring partially flexible buckets. The flexible portion of each bucket was constructed from artificial silk cloth, sewn into a concave shape to allow passive morphing in response to aerodynamic forces.

A V-slot aluminum rig was constructed to support and fix both the turbine and the torque meter. A stainless steel turbine mount equipped with low-friction ball bearings was used to securely attach the turbine to the rig, enabling smooth and stable rotation. **Fig. 5** shows the experimental setup, including the Savonius wind turbine with flexible buckets positioned in front of the wind tunnel, the rig and turbine mounting arrangement, and the torque meter connected to a laptop for data acquisition.

All experiments were conducted with the turbine placed along the centerline at the wind tunnel's exit to ensure symmetrical exposure to the airflow. Mechanical torque was measured using an ATO-TQS-D03 digital rotary torque meter (maximum capacity: 1 N·m; accuracy: 0.00001 N·m), which was mounted directly on the turbine shaft. The torque signal was transmitted to a laptop via an RS485-to-USB converter, and real-time monitoring and recording were performed using dedicated data acquisition (DAQ) software. Wind speed was measured using a vane anemometer (Testo 416), while the turbine's rotational speed was tracked via the integrated tachometer in the torque sensor, also connected to the DAQ system.

Two types of experiments were performed. In the startup performance test, the turbine was released from rest with no applied load, and its free acceleration was monitored until it reached a steady rotational speed. This procedure enabled evaluation of the turbine's self-starting capability under various wind speeds. In the power coefficient measurement, the turbine was first allowed to spin freely until reaching a steady-state tip speed ratio (TSR). A mechanical braking system was then gradually applied to slow the turbine to a complete stop. Throughout this process, torque and rotational speed data were continuously recorded, allowing accurate computation of the instantaneous mechanical power output and, subsequently, the power coefficient at various TSR values.

This experimental setup provided a consistent and repeatable testing environment for comparing the aerodynamic performance of rigid and flexible-bucket Savonius turbines. The results were used to assess the influence of passive flexibility on torque generation, startup behavior, and overall power coefficient.

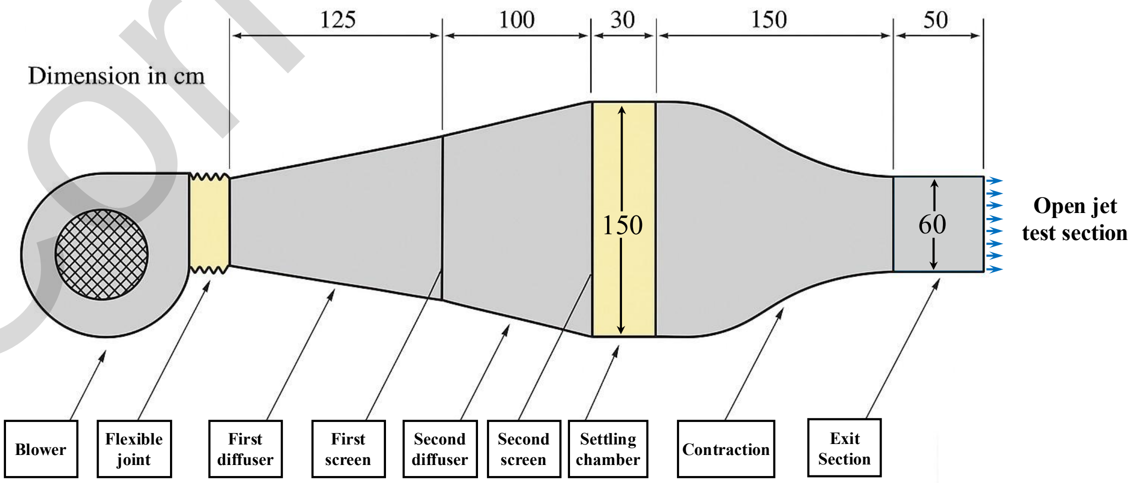

Fig. 4: A schematic of the optimized open-jet wind tunnel at Port Said University's utilized in this work

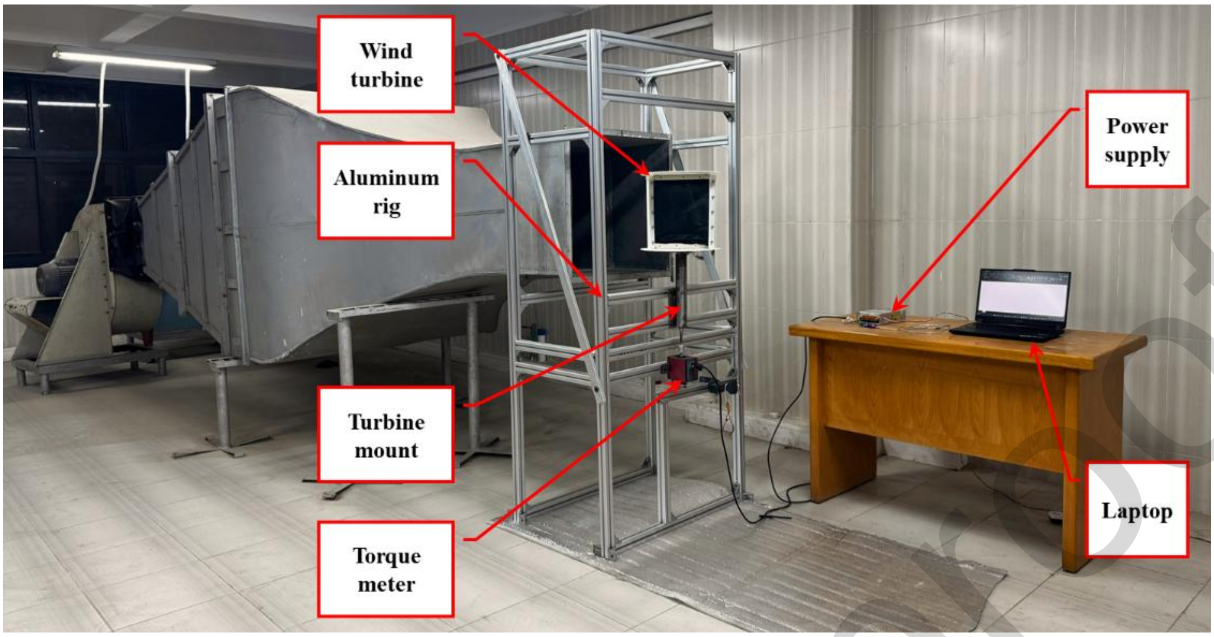

Fig. 5: Experimental setup showing the Savonius wind turbine with flexible buckets positioned in front of the wind tunnel

4. RESULTS AND DISCUSSIONS

4.1.Baseline Performance: Effect of Wind Speed on the Rigid-Bucket Savonius Turbine

The aerodynamic performance of the reference Savonius turbine equipped with fully rigid buckets was assessed under three distinct wind speed conditions—6, 7, and 8 m/s—selected to represent typical low to moderate wind regimes. During the startup phase, the turbine consistently demonstrated its ability to self-initiate rotation without any external assistance, as shown in **Fig. 6**. The time required to reach a stable rotational state varied with wind speed, recorded as approximately 36.3 seconds at both 6 and 7 m/s, and 28.3 seconds at 8 m/s. The corresponding steady-state tip speed ratios (TSR) achieved were approximately 0.98, 1.16, and 1.21, respectively. These results confirm the self-starting capability of the rigid-bucket configuration across a realistic range of operating conditions.

The power output behavior of the turbine is presented in **Fig. 7**, which depicts the variation of the power coefficient (Cp) with TSR for each tested wind speed. The maximum Cp values observed were approximately 8.3%, 11.2%, and 12.2% for wind speeds of 6, 7, and 8 m/s, respectively, indicating a clear trend of increasing energy conversion efficiency with higher wind velocity. Furthermore, the peak power coefficients were found to occur at TSR values of roughly 0.81, 0.88, and 0.90, respectively. This demonstrates that optimal energy extraction is closely associated with the rotational speed relative to the incoming wind. Notably, the turbine exhibited similar performance characteristics at 7 and 8 m/s, with smooth Cp–TSR curves and consistent aerodynamic response. However, at 6 m/s, both the power coefficient and TSR showed a marked decline, indicating reduced efficiency under lower wind conditions. This performance degradation is likely attributed to increased sensitivity to self-starting limitations and aerodynamic inefficiencies associated with low Reynolds number flows.

Accordingly, the 8 m/s case was selected as the reference condition for evaluating the potential performance enhancements introduced by alternative bucket configurations incorporating partial flexibility. This higher wind speed ensures robust and consistent turbine operation, allowing for a more reliable comparison of aerodynamic behavior, power output, and efficiency across different design variants. Subsequent analyses, therefore, focus on assessing the impact of varying flexible and sagitta ratios under this representative operating condition.

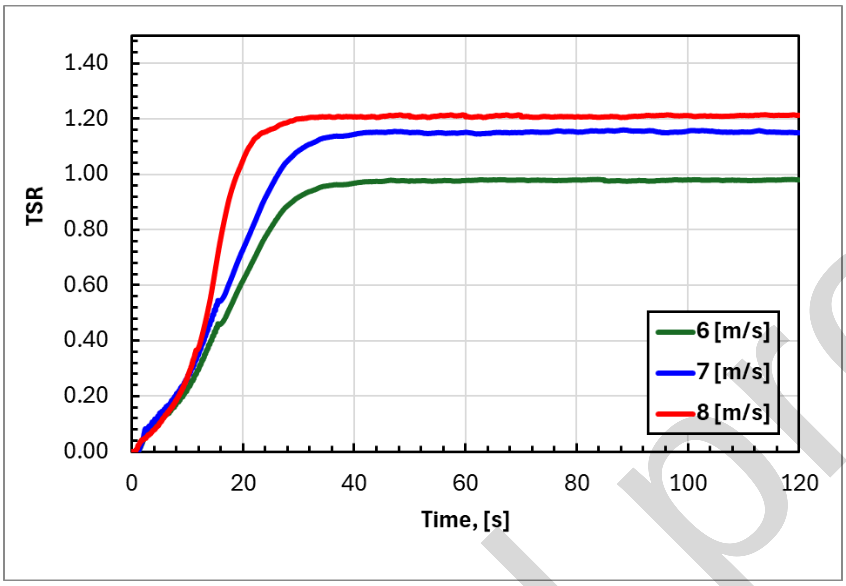

Fig. 6: Startup response of the rigid-bucket Savonius turbine at different wind speeds (6, 7, and 8 m/s)

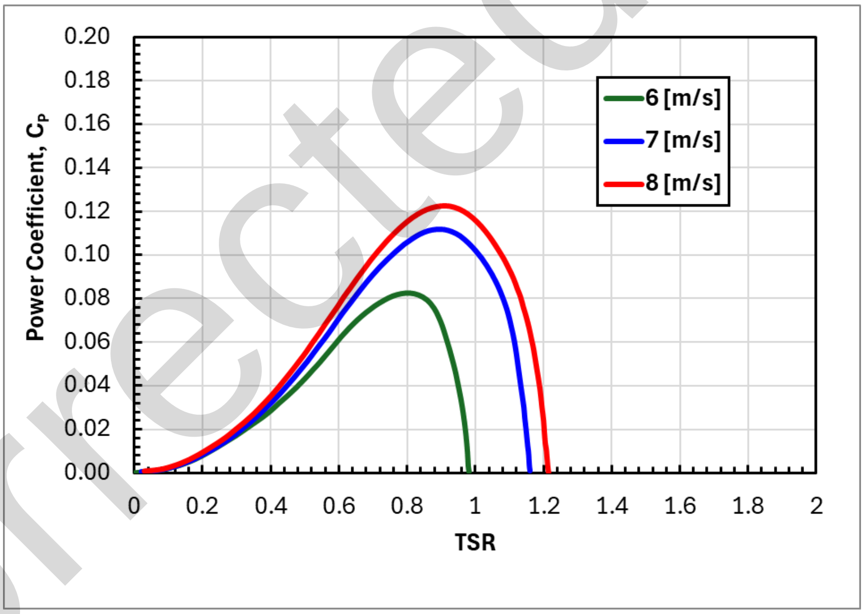

Fig. 7: Variation of power coefficient Cp with tip speed ratio (TSR) for the rigid-bucket Savonius turbine at wind speeds of 6, 7, and 8 m/s

4.2. Performance of Novel Savonius Turbine with Partially Flexible Buckets

This section presents an in-depth examination of how passive flexibility, introduced through partially deformable bucket surfaces, affects the aerodynamic performance of Savonius wind turbines. As outlined in Section 2, the flexible portion of each bucket is characterized by two dimensionless parameters: the Sagitta Ratio (SR), which represents the curvature of the flexible surface, and the Flexible Ratio (FR), which defines the width of the flexible region relative to the overall turbine diameter. The initial phase of this analysis focuses on a constant FR of 0.4, exploring the effects of varying SR values (0.1, 0.2, and 0.3) on both startup behavior and aerodynamic power output. A rigid reference turbine is used as a benchmark, and all experimental data were collected under a steady wind speed of 8 m/s, as justified in Section 4.1.

The startup performance corresponding to FR = 0.4 is presented in **Fig. 8a**. All flexible-bucket configurations successfully initiated rotation, confirming their self-starting capability. However, their startup dynamics were less favorable than the rigid reference turbine. The rigid turbine achieved a steady-state tip speed ratio (TSR) of 1.21 in 28.3 seconds, indicating superior acceleration characteristics. Among the flexible designs, the turbine with SR = 0.2 demonstrated the best performance, reaching a TSR of 1.00 in 28.4 seconds—nearly identical in response time to the rigid turbine but with a slightly reduced final TSR. The configuration with SR = 0.3 followed, attaining a TSR of 0.95 in 42.0 seconds, while the SR = 0.1 design displayed the slowest performance, stabilizing at a TSR of 0.87 in 54.9 seconds. These results suggest that an intermediate curvature, specifically SR = 0.2, provides a favorable balance between passive deformation and aerodynamic drag reduction during startup.

Fig. 8b illustrates the corresponding power performance curves, showing the variation of the power coefficient (Cp) with TSR. The turbine with SR = 0.1 achieved a peak Cp of 7.6% at a TSR of 0.73, while the SR = 0.3 design attained a higher Cp of 9.0% at a TSR of 0.90. Notably, the SR = 0.2 configuration outperformed the other flexible variants, achieving a peak Cp of 9.8% at a TSR of 0.76. In contrast, the rigid reference turbine exhibited the highest aerodynamic efficiency, reaching a peak Cp of 12.2% at a TSR of 0.90. Although the flexible designs did not surpass the rigid reference, the SR = 0.2 case consistently demonstrated competitively close performance.

These results highlight the intricate interplay between flexible canopy curvature and aerodynamic loading. The SR = 0.2 configuration emerged as the most efficient among the flexible designs in both startup and power output phases, suggesting that judicious tuning of passive deformation can significantly enhance performance without compromising structural robustness.

The analysis was further extended by increasing the Flexible Ratio to FR = 0.5, thereby enlarging the deformable region of the bucket. This adjustment was intended to explore whether a broader flexible surface would improve or impair turbine performance. The sagitta ratios examined remained consistent (SR = 0.1, 0.2, and 0.3), and performance was evaluated against the rigid turbine under the same wind conditions.

Startup results for FR = 0.5 are shown in **Fig. 9a**. All configurations demonstrated improved acceleration relative to their FR = 0.4 counterparts. The turbine with SR = 0.2 again showed the most rapid response, reaching a steady-state TSR of 1.15 in 24.8 seconds. This was not only faster than its own FR = 0.4 counterpart but also slightly quicker than the rigid reference. The SR = 0.1 and SR = 0.3 turbines reached TSRs of 1.02 and 1.09 in 27.8 and 27.4 seconds, respectively. These findings indicate that increasing FR to 0.5 enhances startup dynamics, especially when combined with an optimal curvature such as SR = 0.2.

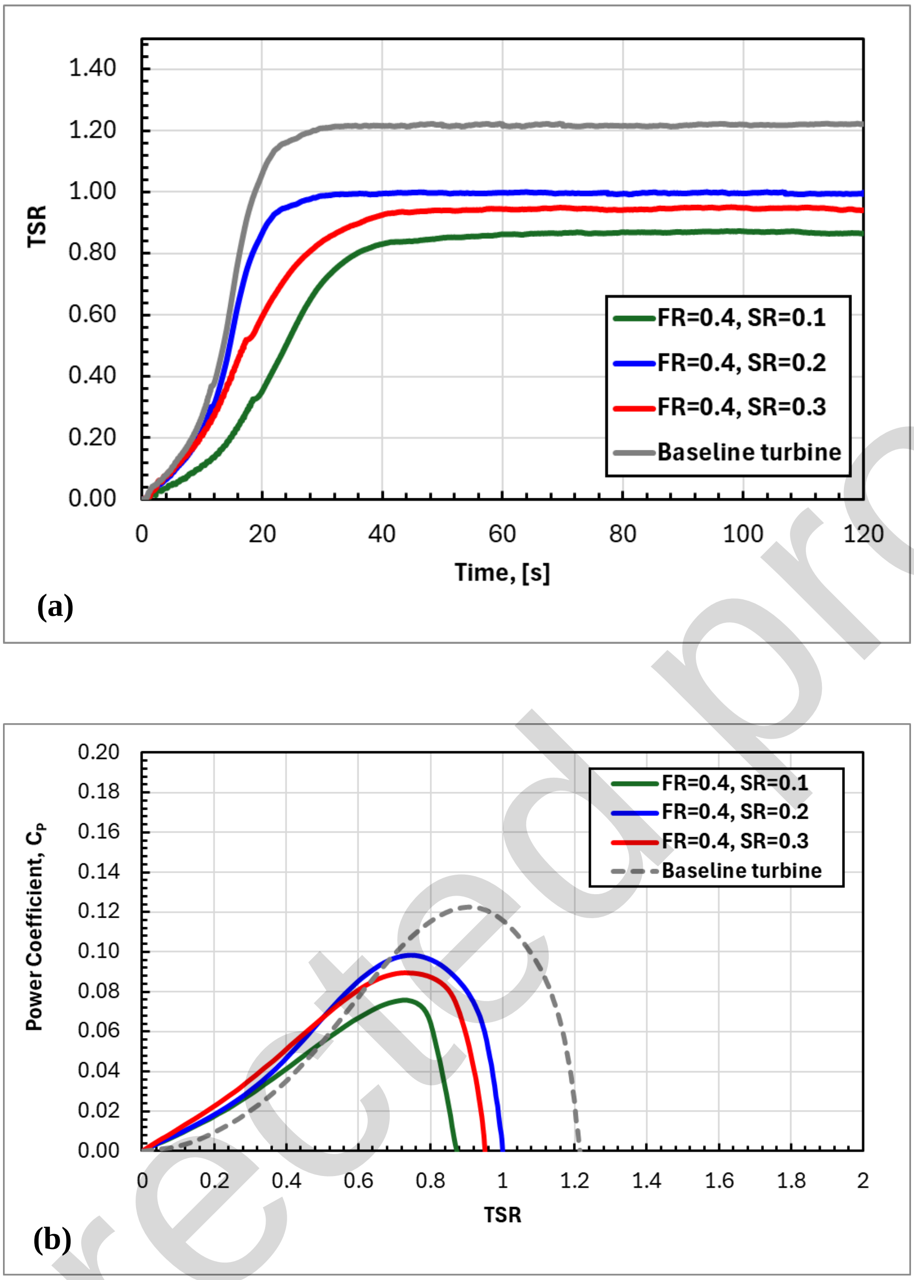

Fig. 8: Comparison of (a) startup response and (b) power coefficient curves of flexible-bucket Savonius turbines with different sagitta ratios (SR = 0.1, 0.2, 0.3) at FR = 0.4 and a wind speed of 8 m/s

Fig. 9b presents the corresponding aerodynamic performance for this set of configurations. The turbine with SR = 0.2 once again led the group, achieving a peak Cp of 12.9% at a TSR of 0.85—slightly surpassing the rigid reference turbine's 12.2% at TSR = 0.90. The SR = 0.3 and SR = 0.1 variants followed with peak Cp values of 10.6% and 9.3% at TSRs of 0.84 and 0.81, respectively. These results support the assertion that moderate flexibility, when coupled with optimal curvature, can yield aerodynamic performance that meets or exceeds that of rigid turbines.

To assess the limits of this trend, the analysis was extended to FR = 0.6, representing the highest level of flexibility in this study. Sagitta ratios of SR = 0.1, 0.2, and 0.3 were again examined and compared to the rigid reference turbine.

The startup behaviors for FR = 0.6 are depicted in **Fig. 10a**. Although all configurations retained self-starting capability, their performance declined relative to lower FR values. The turbine with SR = 0.2 again performed best among flexible designs, reaching a TSR of 1.09 in 34.2 seconds. The SR = 0.3 turbine attained 1.06 in 39.2 seconds, while SR = 0.1 showed the poorest performance, stabilizing at 0.93 in 48.3 seconds. These results suggest that excessive flexibility can introduce adverse effects on startup dynamics, particularly when paired with lower curvature levels.

The power coefficient trends for FR = 0.6 are shown in **Fig. 10b**. The SR = 0.2 configuration maintained its lead, recording a peak Cp of 10.3% at a TSR of 0.89. The SR = 0.3 turbine followed with 9.7% at a TSR of 0.81, and the SR = 0.1 design yielded the lowest Cp of 8.4% at a TSR of 0.78. These outcomes further emphasize that while high flexibility can offer aerodynamic adaptability, it may also dampen performance if not properly balanced with structural and geometric parameters.

To isolate the influence of the Flexible Ratio alone, a focused comparison was conducted at a fixed Sagitta Ratio of SR = 0.2, chosen due to its consistently favorable results. **Fig. 11a and 11b** summarize the startup and aerodynamic performance of turbines with FR values of 0.4, 0.5, and 0.6 at this fixed curvature.

As illustrated in **Fig. 11a**, the turbine with FR = 0.5 demonstrated the fastest startup, reaching a TSR of 1.15 in 24.8 seconds. This outperformed the FR = 0.4 and FR = 0.6 configurations, which reached TSRs of 1.00 and 1.09 in 28.4 and 34.2 seconds, respectively. The results suggest that an intermediate FR value offers the best compromise between aerodynamic responsiveness and structural damping.

The power output curves shown in **Fig. 11b** reinforce this conclusion. The FR = 0.5 turbine reached a peak Cp of 12.9% at a TSR of 0.85, surpassing both FR = 0.4 and FR = 0.6, which recorded 9.8% at a TSR of 0.73, and 10.3% at a TSR of 0.89, respectively. This performance underscores the benefit of using a moderately flexible region with optimal curvature.

In summary, the SR = 0.2 configuration emerged as the most balanced design across all examined levels of FR, delivering consistent startup and aerodynamic performance. In particular, the combination of SR = 0.2 and FR = 0.5 proved to be a standout, offering an effective trade-off between passive adaptability and aerodynamic efficiency. These findings provide compelling evidence for the potential of passively deformable geometries in optimizing Savonius wind turbine performance.

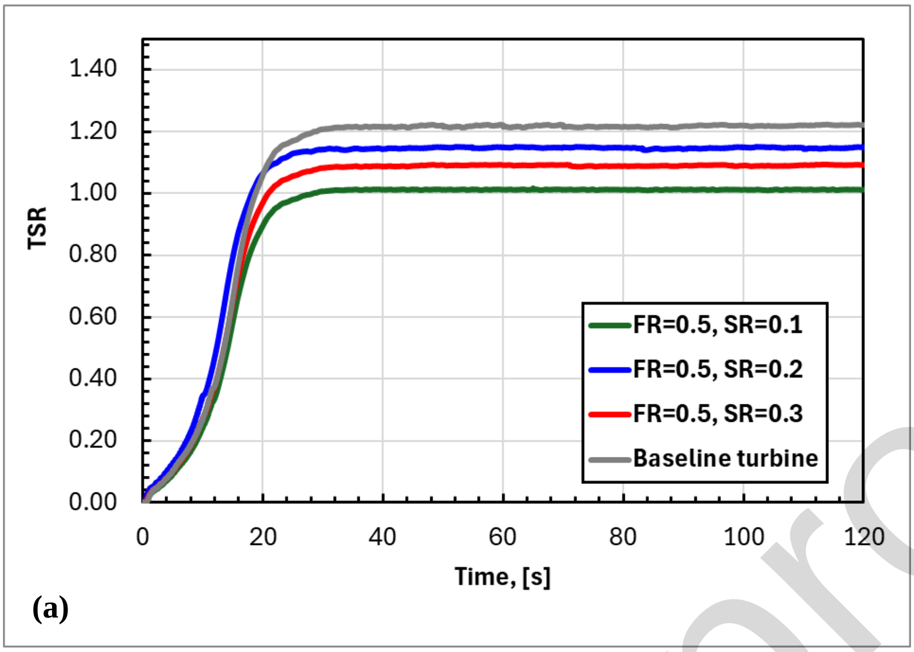

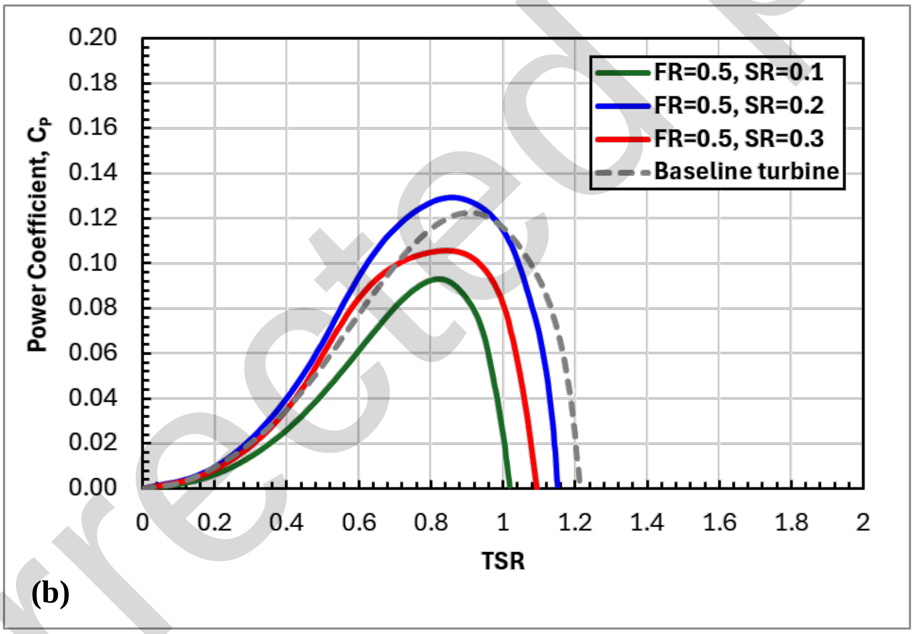

Fig. 9: Comparison of (a) startup response and (b) power coefficient curves of flexible-bucket Savonius turbines with different sagitta ratios (SR = 0.1, 0.2, 0.3) at FR = 0.5 and a wind speed of 8 m/s

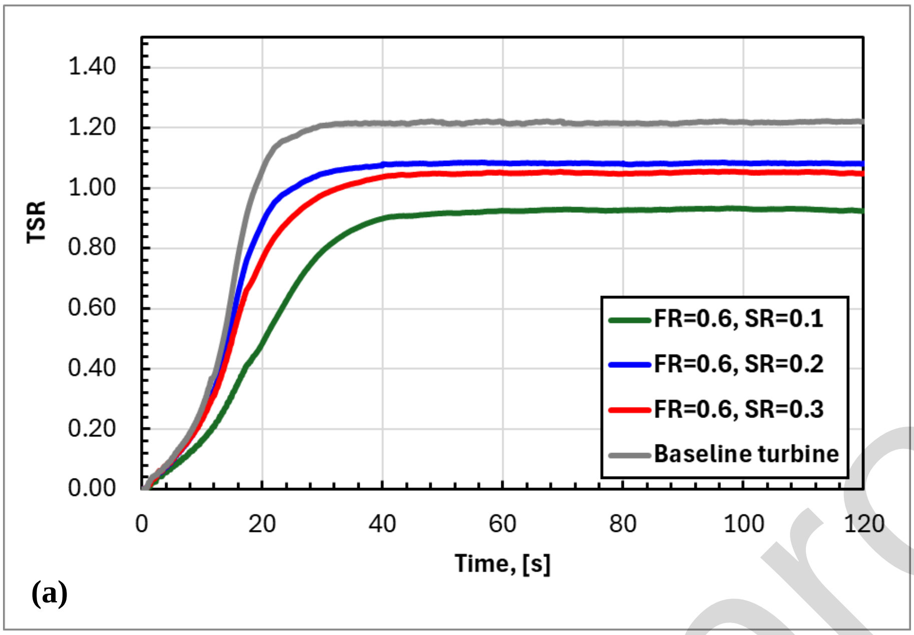

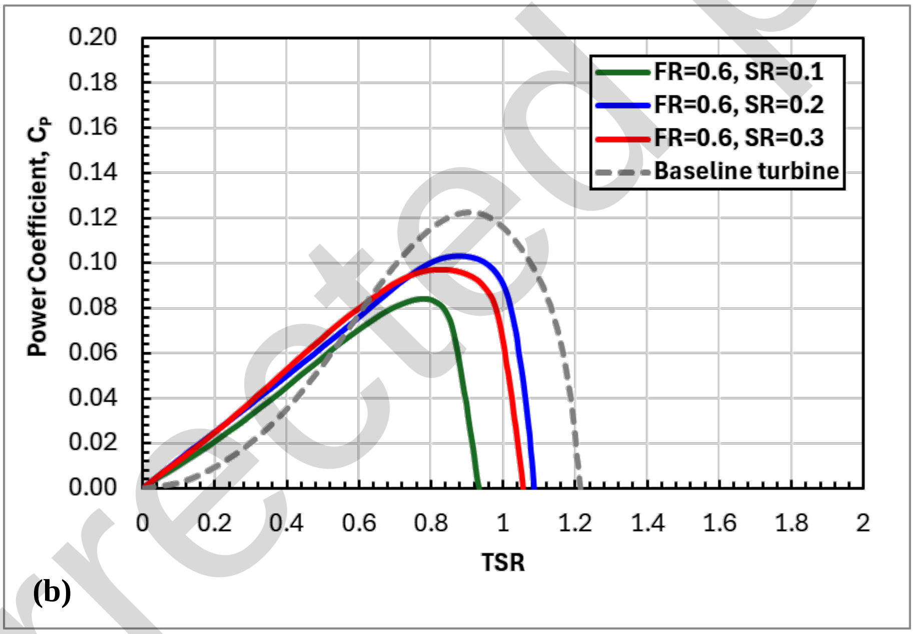

Fig. 10: Comparison of (a) startup response and (b) power coefficient curves of flexible-bucket Savonius turbines with different sagitta ratios (SR = 0.1, 0.2, 0.3) at FR = 0.6 and a wind speed of 8 m/s.

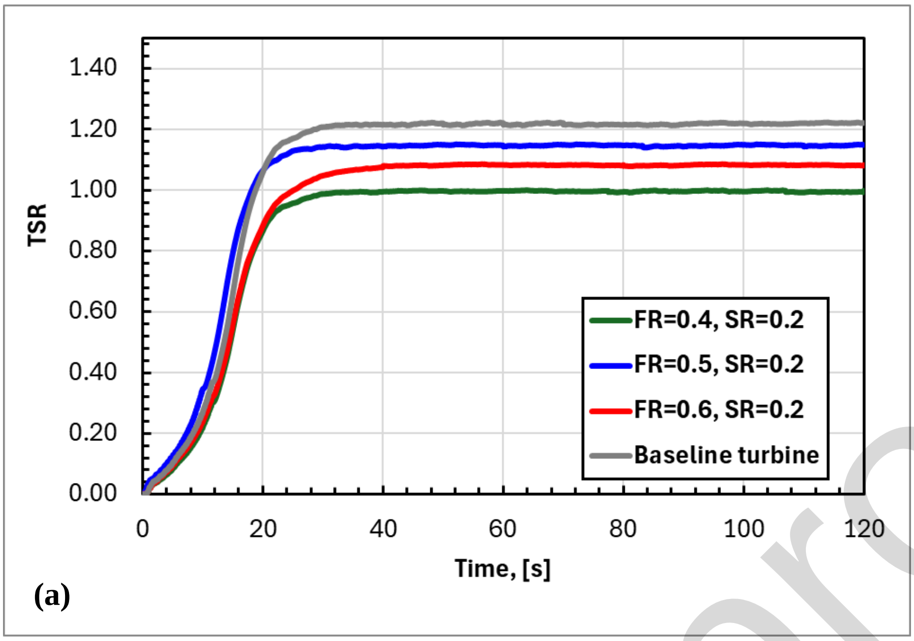

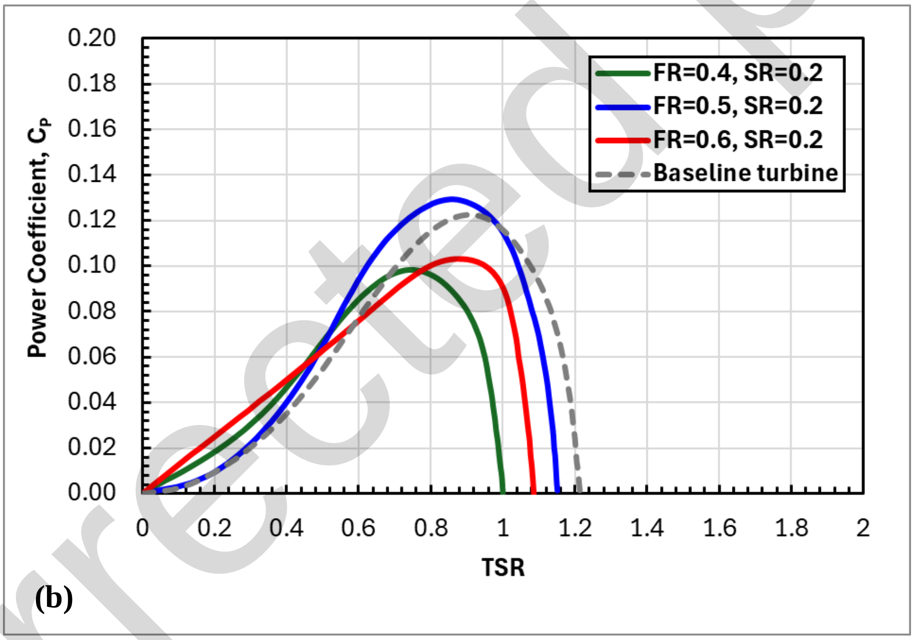

Fig. 11: Comparison of (a) startup response and (b) power coefficient curves of flexible-bucket Savonius turbines with sagitta ratios SR = 0.2 with different Flexible ratios (FR = 0.4, 0.5, 0.6) and a wind speed of 8 m/s.

A comprehensive summary of the aerodynamic performance of flexible-bucket Savonius turbines is provided in **Fig. 12 and Tables 1 and 2**. These visualizations collectively highlight the influence of varying Sagitta Ratios (SR) and Flexible Ratios (FR) on both startup characteristics and power conversion efficiency under a constant wind speed of 8 m/s. **Fig. 12** illustrates the trend of maximum power coefficients across different configurations, while **Table 1** presents the corresponding maximum tip speed ratios (TSRs) and steady-state times. **Table 2** complements this by detailing the peak Cp values and their associated TSRs for each configuration. The rigid-bucket turbine configuration is included in all comparisons to serve as a baseline reference for performance evaluation.

Taken together, the results underscore the critical role of passive deformation in shaping Savonius turbine performance. Among the tested parameters, the SR = 0.2 configuration consistently demonstrated the best balance between aerodynamic efficiency and startup responsiveness across all FR levels. Notably, the turbine with FR = 0.5 and SR = 0.2 not only outperformed all flexible configurations but also surpassed the rigid turbine in key performance metrics. It achieved a peak power coefficient (Cp) of 12.9%, compared to 12.2% for the rigid turbine, reflecting an improvement of approximately 5.7% in aerodynamic efficiency. Additionally, it reached steady-state rotation in just 24.8 seconds, which is 12.4% faster than the 28.3 seconds required by the rigid design. This indicates a significant enhancement in startup dynamics, reducing the mechanical stress and energy loss typically associated with prolonged acceleration phases.

Such improvements validate the hypothesis that a carefully tuned combination of curvature and deformable surface extent can enhance turbine behavior without compromising structural integrity. The consistent superiority of the SR = 0.2 design across varying FR values further reinforces its robustness as an optimal passive flexibility configuration. To further refine this promising performance envelope, a dedicated optimization study—either through advanced experimental investigations or high-fidelity CFD simulations—is recommended. This would help identify the precise FR–SR combinations that yield the most effective trade-offs between aerodynamic output, structural resilience, and manufacturing feasibility. Such insights offer a valuable design framework for enhancing the viability and efficiency of vertical-axis wind turbines, particularly in low-to-moderate wind speed environments.

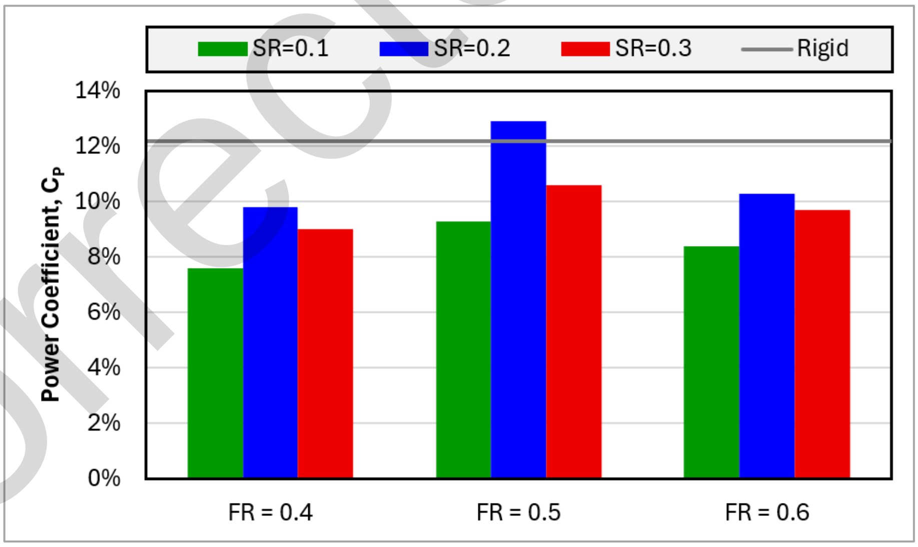

Fig. 12: Maximum power coefficient (Cp) values for rigid and flexible-bucket Savonius turbines across different Sagitta Ratios (SR = 0.1, 0.2, 0.3) and Flexible Ratios (FR = 0.4, 0.5, 0.6) at a wind speed of 8 m/s. The rigid configuration serves as a performance benchmark

Table 1: Summary of maximum tip speed ratios and steady-state times for flexible and rigid Savonius turbines at 8 m/s, evaluated across different Sagitta Ratios (SR) and Flexible Ratios (FR)

Configuration	Maximum TSR			Steady-State Time (s)		
	SR=0.1	SR=0.2	SR=0.3	SR=0.1	SR=0.2	SR=0.3
FR = 0.4	0.87	1	0.95	54.9	28.4	42
FR = 0.5	1.02	1.15	1.09	27.8	24.8	27.4
FR = 0.6	0.93	1.09	1.06	48.3	34.2	39.2
Rigid		1.21			28.3	

Table 2: Comparison of peak power coefficients and corresponding tip speed ratios for flexible and rigid Savonius turbines at 8 m/s.

Configuration	Maximum Cp (%)			TSR at Maximum Cp		
	SR=0.1	SR=0.2	SR=0.3	SR=0.1	SR=0.2	SR=0.3
FR = 0.4	7.60%	9.80%	9.00%	0.73	0.76	0.9
FR = 0.5	9.30%	12.90%	10.60%	0.81	0.85	0.84
FR = 0.6	8.40%	10.30%	9.70%	0.78	0.89	0.81
Rigid		12.20%			0.9	

SUMMARY AND CONCLUSIONS

This study has demonstrated that integrating passive flexibility into Savonius wind turbine buckets can significantly improve aerodynamic performance, especially under low wind speed conditions. By introducing deformable fabric-based bucket sections parameterized by sagitta ratio (SR) and flexible ratio (FR), the research confirmed that optimized passive morphing enhances both startup dynamics and energy conversion efficiency. Notably, the best-performing configuration—SR = 0.2 and FR = 0.5—achieved a peak power coefficient (Cp) of 12.9%, surpassing the rigid baseline Cp of 12.2%. Moreover, this configuration reached steady-state rotation in just 24.8 seconds, compared to 28.3 seconds for the rigid turbine, indicating superior responsiveness.

Experimental results revealed that while all flexible designs retained self-starting capability, excessive flexibility or suboptimal curvature led to reduced performance. Thus, the study highlights the critical importance of geometric tuning in achieving a favorable balance between adaptability and aerodynamic efficiency.

These findings validate the hypothesis that passive morphing can enhance the performance of drag-based turbines without introducing mechanical complexity or significant cost. The proposed design—employing artificial silk fabric for deformation—offers a structurally simple and scalable solution for decentralized wind energy generation, especially in urban or low-wind environments.

Future work should focus on detailed optimization of the SR–FR design space using advanced simulations and long-term durability testing under real-world conditions. Such research will be essential to fully harness the potential of flexible wind turbine geometries and advance the broader adoption of sustainable wind energy technologies.

ACKNOWLEDGMENTS

Gratitude is extended to the Academy of Scientific Research and Technology (ASRT) for their support, provided through the ASRT Green Fund: Climate Change Adaptation and Nature Conservation, for the project titled "Green innovative forced ventilation system powered by wind turbines to reduce heat stress from climate change in residential and industrial buildings".

CONFLICT OF INTEREST

The authors have no financial interest to declare in relation to the content of this article.

REFERENCES

[1] D. H. Didane, M. R. Behery, M. Al-Ghriybah, and B. Manshoor, “Recent Progress in Design and Performance Analysis of Vertical-Axis Wind Turbines—A Comprehensive Review,” Processes, vol. 12, no. 6, p.1094, May 2024.

[2] F. Goudarzi et al., “A critical review of vertical axis wind turbines for urban applications,” Renewable and Sustainable Energy Reviews, vol. 89, pp. 281–291, Jun. 2018.

[3] N. Alom and U. K. Saha, “Aerodynamic analysis of a 2-stage elliptical-bladed Savonius wind rotor: Numerical simulation and experimental validation,” International Journal of Green Energy, pp. 1–14, Mar. 2023.

[4] M. H. F. Mahizam, W. S. Chang, E. Fatahian, F. Ismail, and M. H. H. Ishak, “Improving Savonius turbine efficiency with splitter and barrier cylinder deflector design: A Taguchi method study,” The Physics of fluids, Nov. 2023.

[5] A. G. Chitura, P. Mukumba, and N. Lethole, “Enhancing the performance of Savonius wind turbines: A review of advances using multiple parameters,” Energies, vol. 17, no. 15, p. 3708, 2024.

[6] Rizk, M. A., & Nasr, K. (2023). Computational fluid dynamics investigations over conventional and modified Savonius wind turbines. Heliyon, 9(6).

[7] A. S. Saad, A. Elwardany, I. I. El-Sharkawy, S. Ookawara, and M. Ahmed, “Performance evaluation of a novel vertical axis wind turbine using twisted blades in multi-stage Savonius rotors,” Energy Convers. Manage., vol. 235, p. 114013, 2021.

[8] D. Altan and M. Atilgan, “An experimental and numerical study on the improvement of the performance of Savonius wind rotor,” Energy Convers. Manage., vol. 49, no. 12, pp. 3425–3432, 2008.

[9] E. Fatahian, F. Ismail, M. H. H. Ishak, and W. S. Chang, “An innovative deflector system for drag-type Savonius turbine using a rotating cylinder for performance improvement,” Energy Convers. Manage., vol. 257, p. 115453, 2022.

[10] W. Yahya, K. Ziming, W. Juan, M. S. Qurashi, M. Al-Nehari, and E. Salim, “Influence of tilt angle and the number of guide vane blades towards the Savonius rotor performance,” Energy Rep., vol. 7, pp. 3317–3327, 2021.

[11] A. Alaimo, A. Esposito, A. Milazzo, C. Orlando, and F. Trentacosti, “Slotted blades Savonius wind turbine analysis by CFD,” Energies, vol. 6, no. 12, pp. 6335–6351, 2013.

[12] R. Wahyudi, D. M. Kurniawati, and A. Djafar, “Effect of slotted angle on Savonius wind turbine performance,” Adv. Sci. Technol., vol. 104, pp. 83–88, 2021.

[13] D. Tjahjana, Z. Arifin, S. Suyitno, W. E. Juwana, A. R. Prabowo, and C. Harsito, “Experimental study of the effect of slotted blades on the Savonius wind turbine performance,” Theor. Appl. Mech. Lett., vol. 11, no. 3, p. 100249, 2021.

[14] R. Kumar and A. Kumar, “Optimization of slot parameters for performance enhancement of slotted Savonius hydrokinetic turbine using Taguchi analysis,” Renew. Energy, vol. 237, p. 121608, 2024.

[15]Y. S. Indartono, I. Farozan, and G. T. Fauzanullah, "Experimental study into the effect of multi-staging and check valve addition on the performance of Savonius wind rotors with modified-Bach blade," Int. J. Technol., vol. 16, no. 2, pp. 602–612, 2025

[16] M. Amiri and M. Anbarsooz, "Improving the energy conversion efficiency of a Savonius rotor using automatic valves," J. Sol. Energy Eng., vol. 141, no. 3, p. 031017, 2019.

[17] A. Zereg, M. T. Bouzaher, M. Aksas, and N. Lebaal, "Performance enhancement of Savonius wind turbine through partially deformable blades," Int. J. Simul. Multidiscip. Des. Optim., vol. 15, p. 8, 2024.

[18] D. Obidowski, K. Sobczak, K. Jóźwik, and P. Reorowicz, Vertical axis wind turbine with a variable geometry of blades, European Patent EP3702610A1, Sep. 2, 2020.

[19]] K. Sobczak, D. Obidowski, P. Reorowicz, and E. Marchewka, "Numerical investigations of the Savonius turbine with deformable blades," Energies, vol. 13, no. 14, p. 3717, 2020.

[20] E. Marchewka, K. Sobczak, P. Reorowicz, D. Obidowski, and K. Jóźwik, "Influence of tip speed ratio on the efficiency of Savonius wind turbine with deformable blades," in J. Phys.: Conf. Ser., vol. 2367, no. 1, p. 012003, Nov. 2022.

[21] M. T. Bouzaher and B. Guerira, "Impact of flexible blades on the performance of Savonius wind turbine," Arab. J. Sci. Eng., vol. 47, pp. 15,365–15,377, 2022.

[22] A. S. Abdelhamed, Y. E. S. Yassen, and M. M. ElSakka, "Design optimization of three-dimensional geometry of wind tunnel contraction," Ain Shams Eng. J., vol. 6, no. 1, pp. 281–288, 2015.

[23] A. S. Singhal, S. V. Jain, R. N. Patel, V. Parmar, and R. Pathak, "On the enhancement of acceptable blockage of open jet wind tunnel by employing modifications based on concepts of boundary layer and jet flow for testing of aero-rotors," Results Eng., vol. 24, p. 102934, 2024.